DRAFT

Support Tube FEA Modeling Summary

1.0 Introduction

This document describes the initial vibration results for FEA analysis performed on the Pixel Support Tube (PST) composite installation structure. The structure is initially analyzed without additional mass (i.e. Pixel and services structures) as these are thought to be primarily mechanically independent (due to fixation schemes). Later, the models are examined with a distributed service mass incorporated into the shell. The PST is modeled with and without several mechanical structures that are attached to it, in order to quantify the stiffening effects of these components. Different material properties are also investigated. For instance, a fiberglass forward tube section is investigated in response to concerns about loads the PST could apply to surrounding detectors (namely the SCT). In all analyses, the four lowest modes were computed using ANSYS FEA software.

2.0 Geometry

The PST consists of three individual segments that are bolted together through stiffening flanges: 1 barrel, and 2 forwards. For modeling purposes, the flange connections are assumed to be perfect, and no bolt holes are included. All bonded joints (including flange to tube connections) are modeled as perfectly welded interfaces, with no glue properties or elements. A schematic of the PST model is shown in Figure 1.

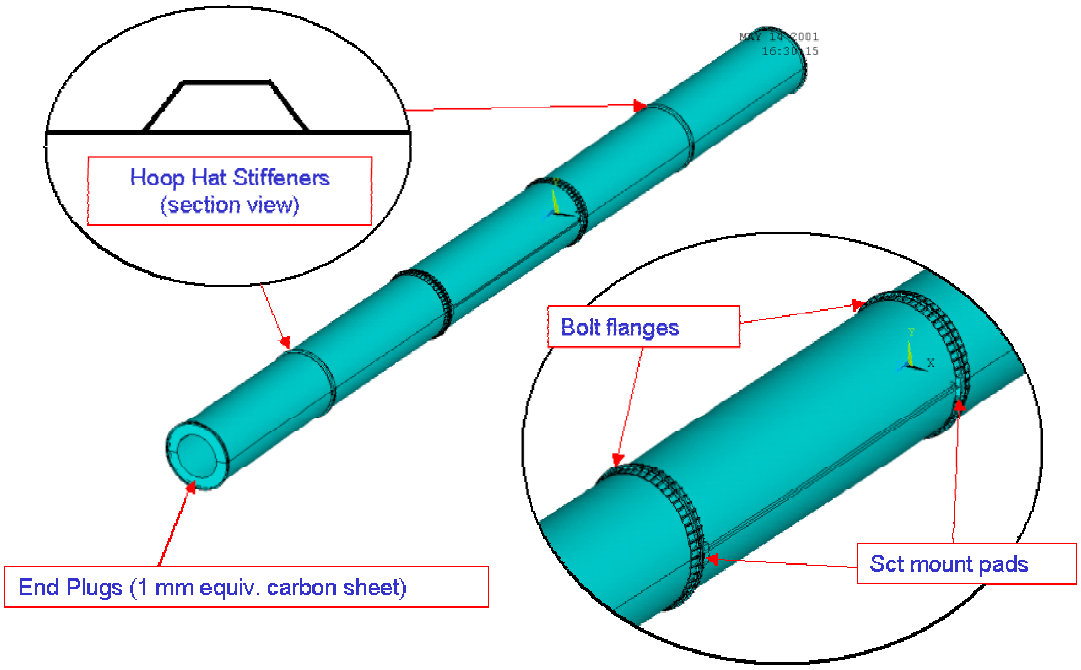

Figure 1. Important features in the PST FEA model (longitudinal ribs have not been shown).

3.0 Constraints

The PST is modeled with different constraint conditions in order to evaluate the need for specific types of fixation to the surrounding detectors (outside of the pixel detector). The baseline fixation scheme is shown in Figure 2, along with the support conditions that were examined during analysis. In particular, the effect of end-fixation at the forward tubes (on extreme sides A and C) is analyzed by removing the vertical freedom on both sides, and the X direction freedom on one side of the PST. The effect of fixing across the diameter of the barrel tube is also examined. Also, it should be noted that all constraints are applied to small areas or lines on the PST flanges. These constraints do not allow free rotation, and thus cannot be considered "simple" in the classical beam sense. This support condition more closely models the proposed mounting flexures than constraints that allow free rotation.

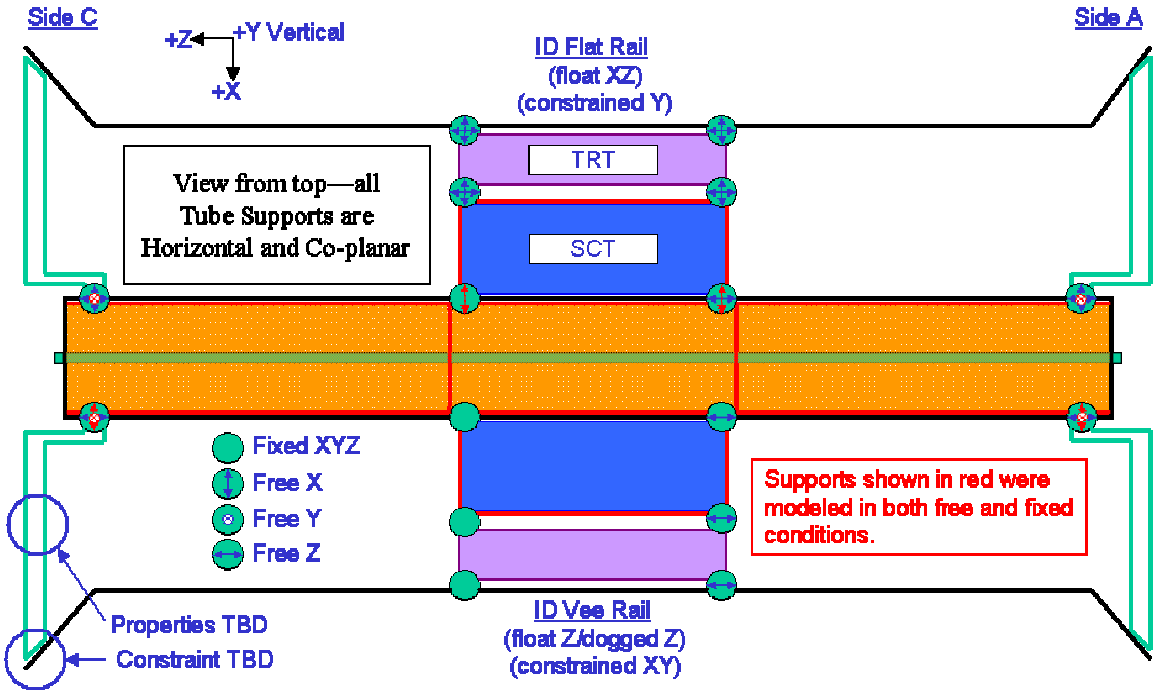

Figure 2. PST baseline support conditions showing constraints that were varied in the FEA model (in red).

4.0 Model Properties

The PST model consists of either 2 or 3 types of materials. The barrel shell, or tube, structure is assumed to be constructed of high modulus (HM) graphite fiber (E=420 GPa) in a cyanate ester resin matrix, with 8 plies arranged in a quasi-isotropic manner ($[0/90/+45/-45]_S$). This layup achieves an isotropic modulus of approximately 98 GPa. The forward shells are composed of either HM graphite or quartz glass fiber; the later gives a quasi-isotropic modulus of 21 GPa given a fiber modulus of 91 GPa. Stiffeners and ribs in the forward sections are assumed to be HM graphite in all cases. The flange is first investigated as a molded and machined PEEK (polyethyletherketone) structure, and then later as a carbon structure comprised of quasi-isotropic ultra high modulus (UHM)

graphite (E=560 GPa) in a cyanate ester matrix, resulting in a bulk modulus of 126 GPa. In all cases, materials are modeled as either shells or solids, with isotropic properties and linear behavior. For the cases where service mass is included in the analysis, the material densities of the forward shells are increased in order to account for the added mass. A summary of all model material properties is given in Table 1.

Table 1. FEA Material Properties.

Material Model	Material Location	Fiber Modulus (GPa)	Bulk Modulus (GPa)	Density (kg/m^3)
High Mod. Carbon	Shell, Hat Stiffeners	420	98	1650
Ultra High Mod. Carbon	Flanges (Option 1)	560	126	1650
PEEK (graphite filled)	Flanges (Option 2)	N/A	3.5	1500
Glass (Quartz)	Forward Shells	91	21	1800
HM Carbon (incl. service mass)	Forward Shells	420	98	12300
Glass (incl. service mass)	Forward Shells	91	21	12450

5.0 Analysis Cases

The primary free variables in this analysis study were as follows:

- Flange Material (PEEK or Carbon Fiber)
- Longitudinal Ribs
- Hoop Stiffeners (in Forwards)
- End Plug (PP1 panel)
- Flange Shape
- Barrel Constraints (ties across SCT diameter)
- Service Mass (incorporated in forward shell material)
- Fiberglass Forward Shells
- Forward End Constraints*

*The issue of using constraints at the forward ends of the PST reflects a fundamental change in support scheme, so *most* model cases were run with both fixed and free forward ends.

6.0 Results

The results are presented in a stepwise fashion, illustrating the progression of the PST design. Each result section presents the inclusion of one of the above design elements, showing why it was either retained or rejected in subsequent iterations.

6.1 Case 1 - Flange Material (PEEK or Carbon Fiber)

The initial baseline PST model included PEEK flanges (for ease of manufacturing) and longitudinal ribs along the entire structure (to combat the anticipated cantilever bending modes) located at the tops and bottoms of the tubes (see Figure 1). The lowest modes all turned out to be shell modes, however, emphasizing that the flange stiffness was much more important than previously appreciated (even when the forward ends of the PST are not constrained). Changing the flange material to isotropic carbon fiber (without changing the shape, which is somewhat non-physical, yet a good comparison) improved the vibrational stability substantially, as shown in Results Table 1. Note that the forward ends, when "fixed", are fixed only in radial dimensions (XY).

Results Table 1. Effect of Carbon vs. PEEK Flanges.
(Shell modes in italics, cantilever modes in bold)

Model Description	Free Forwards				Fixed Forwards			
	Mode 1	Mode 2	Mode 3	Mode 4	Mode 1	Mode 2	Mode 3	Mode 4
PEEK Flanges	*8.9*	*11.9*	*17.9*	*26*	*12.9*	*13.7*	*18*	*42.1*
Carbon Flanges	*24.5*	*41.2*	*61.5*	*65.6*	*54.7*	*55.6*	*69.9*	*72.8*

Since the vibrational improvement in going to carbon flanges is so noticeable (at least a factor of 3, depending on forward fixation) it was decided that the PST required this design element, and all further analyses assume carbon flanges.

6.2 Case 2 - Longitudinal Ribs

The indication that shell stiffness was absolutely dominating PST vibrational behavior led to immediate questioning of whether longitudinal ribs were necessary. The ribs increase the overall PST bending inertia by a factor of 2, but also increase the shell mass by 50%, see Table 2.

Table 2. Longitudinal Rib Comparison for PST.

PST Rib Comparisons	Area (mm^2)	Inertia (mm^4)
PST Tube	726	1.93E+07
PST Ribs (6)	360	1.92E+07
Tube + Ribs	1086	3.85E+07

Analysis showed that, as suspected, the longitudinal ribs did almost nothing to raise PST frequencies. In fact, removing the ribs *raised* the lowest frequencies marginally, see Results Table 2. Although bending modes were observed in the higher orders for the free-ended model, the lowest modes remained shell modes, and so it was decided to remove ribs from the PST design.

Results Table 2. Effect of Longitudinal Ribs.
(Shell modes in italics, cantilever modes in bold)

Model Description	Free Forwards				Fixed Forwards			
	Mode 1	Mode 2	Mode 3	Mode 4	Mode 1	Mode 2	Mode 3	Mode 4
With Ribs	*24.5*	*41.2*	*61.5*	*65.6*	*54.7*	*55.6*	*69.9*	*72.8*
Without Ribs	*25.8*	*44*	**55.9**	**62.4**	*58.5*	*59.2*	*67.9*	*68.5*

6.3 Case 3 - Hoop Stiffeners and End Plugs (PP1)

In addressing the problem of PST shell stiffness, it was obvious that increased sections in the tube were important, particularly along the forwards. The option of a cored structure for the PST shell was considered, but it would more than double mass and cost. The simpler approach was to incorporate circumferential ribs, or "hoops", located at the midpoints of the forwards. In addition, it was realized that the PP1 panels (otherwise known as endplugs) would also add radial stiffness to the PST, and thus these were included in the model (whereas they had been omitted before). This load case was only examined for fixed forward ends, however, so only these results are shown in Results Table 3 and Figure 3.

Results Table 3. Effect of Hoops and End Plugs.
(Shell modes in italics, cantilever modes in bold)

Model Description	Free Forwards				Fixed Forwards			
	Mode 1	Mode 2	Mode 3	Mode 4	Mode 1	Mode 2	Mode 3	Mode 4
Without	*25.8*	*44*	**55.9**	**62.4**	*58.5*	*59.2*	*67.9*	*68.5*
With Hoops and End Plugs	N/A	N/A	N/A	N/A	*64*	*114.6*	*116.5*	*117.9*

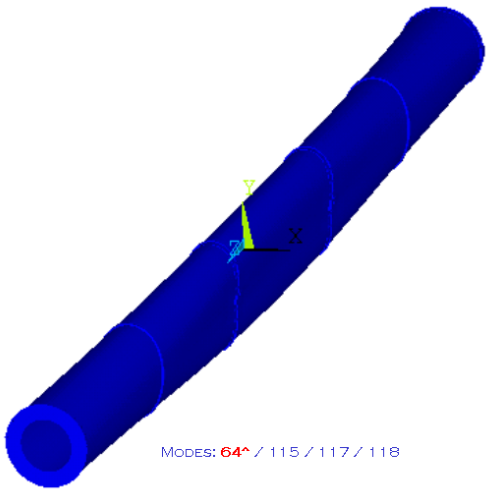

Results Figure 3. Effect of Hoops and End Plugs.

The most notable aspect of the results from this load case is that the fundamental frequency is not increased very substantially (only about 10%). However, looking at the higher order modes (HOM's) it can be seen that they are all increased by almost a factor of 2, to well above 100 Hz (the nominal design criteria). Additionally, it is

evident that the lowest mode is caused by a diaphragm type motion of the entire tube, allowed by the lack of constraints across the PST diameter at the SCT barrel. Constraining the PST across the diameter in addition to increasing the barrel flange thicknesses would raise the fundamental frequency, while causing no decrease in HOM's, thereby reaching a tube with fundamental frequency nearer to, or above, 100 Hz.

6.4 Case 4 – Flange Shape

The initial flange shape chosen for the PST was a simple ribbed annulus, with the goal that it would be machined from a large block of PEEK. Even after rejecting PEEK as the potential flange material, the shape was retained in order to easily judge the effect of changing material properties alone. Since that time, the requirements for the flange have changed (given mounting and gas sealing issues) and a fabrication scheme has been developed. The current flange design utilizes repeated carbon fiber building blocks that are integrated into a bonded assembly, as shown in Figure 3.

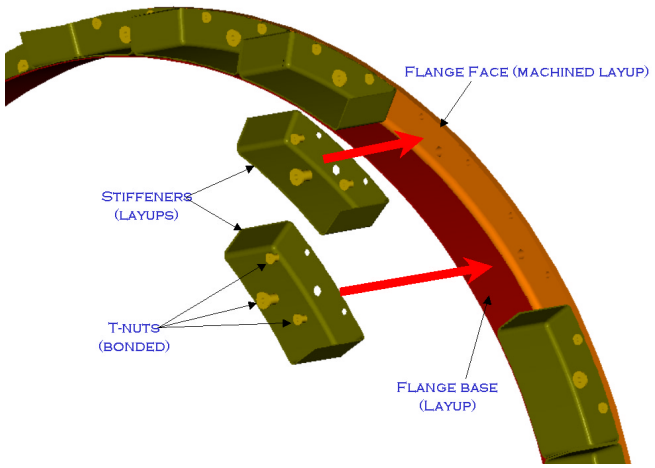

Figure 3. Proposed Carbon Fiber Flange Design.

Results Table 4. Effect of Flange Shape.
(Shell modes in italics, cantilever modes in bold)

Model Description	Free Forwards				Fixed Forwards			
	Mode 1	Mode 2	Mode 3	Mode 4	Mode 1	Mode 2	Mode 3	Mode 4
Initial Flange Shape	N/A	N/A	N/A	N/A	*64*	*114.6*	*116.5*	*117.9*
Carbon Flange Concept	**31.4**	**48.4**	*55.3*	*62.2*	*88.7*	*118.6*	*119*	*123.6*

The assembled shape of this new flange design was modeled as a solid with isotropic properties, which approximates the use of quasi-isotropic laminates in the real assembly. This design has higher stiffness than the original shape, and this stiffness can be seen in the vibrational results (Results Figure 4) as the fundamental frequency is increased by 38%. As in load case 3, the free-ended version of the model with original flange shape was not run. Also, the same diaphragm type mode can be seen; although its frequency is higher, it is still not above the desired 100 Hz threshold.

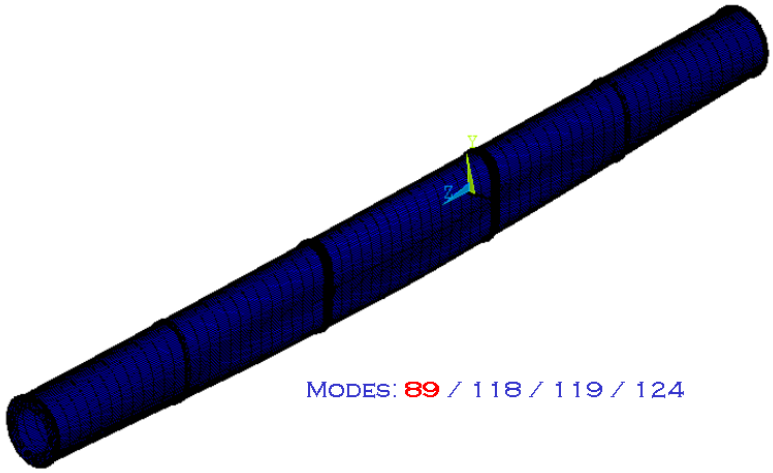

Results Figure 4. Effect of Flange Shape.

6.5 Case 5 – Constraining Across the Barrel (SCT Diameter)

The shape of the lowest mode from the previous analysis leads directly to the hypothesis that constraining the PST across the barrel of the SCT would eliminate the diaphragm type motion observed. Analysis results, Results Table 5, show that this is indeed the case, raising the fundamental frequency to well above 100 Hz, and moving all modes to high frequency shell motion in the forwards, Results Figure 5.

Results Table 5. Effect of Diametral Constraints at SCT Barrel.
(Shell modes in italics, cantilever modes in bold)

Model Description	Free Forwards				Fixed Forwards			
	Mode 1	Mode 2	Mode 3	Mode 4	Mode 1	Mode 2	Mode 3	Mode 4
No Barrel Constraints	31.4	48.4	55.3	62.2	*88.7*	*118.6*	*119*	*123.6*
Barrel Constr. Across SCT	51.3	53.8	55.3	62.2	*118.8*	*119*	*123.6*	*123.7*

Little mention has been made thus far about the effect of forward end freedom, although results are tabulated for most load cases. In general, it has always been perceived that allowing this degree of freedom is unwise. From the results shown thus far, it can be seen that freeing the forward ends lowers frequency by factors of 2 to 3. Introducing service masses into the forwards will only exacerbate this difference, and is thus thought to be unacceptable. Analysis results for the free-ended analysis cases are therefore presented primarily for comparison purposes.

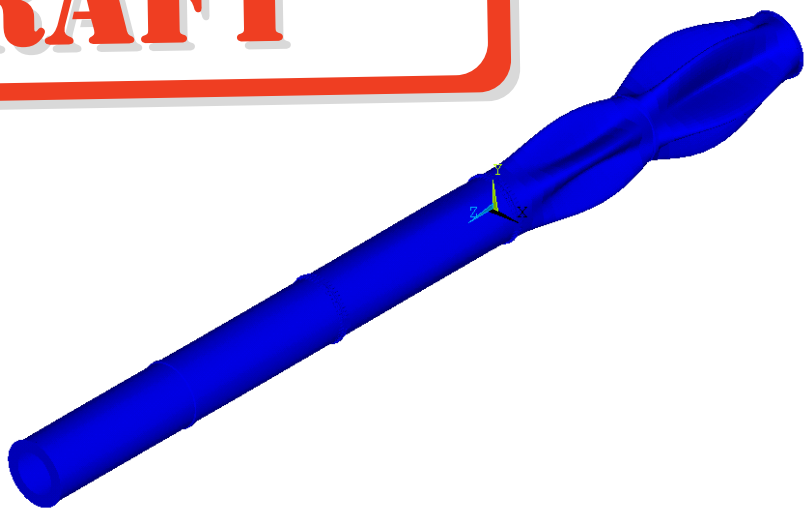

Results Figure 5. Effect of Diametral Constraints at SCT Barrel.

6.6 Case 6 – Effect of Service Mass in the Forwards

Once the PST had been nominally optimized to fundamental frequencies above 100 Hz, it was decided to incorporate service masses in the model. Originally, it had been desired to model the entire service structure in connection with the PST itself. However, this model is extremely large, and the service mass structure has been constantly changing. For these reasons, the service masses were incorporated into the shell material densities (given in Table 1). Since this approximation adds mass, but no stiffness, it yields the most conservative results. The service masses are initially modeled at 13 kg per side (approximately the mass of services on the side *opposite* the b-layer). Since this is *not* conservative, models will soon be run with a higher, more accurate service mass of 17 kg per side. It should be noted, however, that since the service structure is currently under development, a final accounting of all service masses will need to be made before an accurate assessment of the effect on PST stiffness can be judged.

Results Table 6. Effect of Service Mass in the Forwards.
(Shell modes in italics, cantilever modes in bold)

Model Description	Free Forwards				Fixed Forwards			
	Mode 1	Mode 2	Mode 3	Mode 4	Mode 1	Mode 2	Mode 3	Mode 4
No Service Mass	51.3	53.8	55.3	62.2	*118.8*	*119*	*123.6*	*123.7*
Service Mass (13 kg)	**26.4**	**27.7**	**28.6**	**32.3**	*53.1*	*53.2*	*54.2*	*54.2*

Initial results in Results Table 6 show that the addition of service masses decreases the fundamental frequencies across the board by a factor of almost 2 or more. As might be expected, all modes for the free-ended case are beam modes (cantilever bending) while all modes for the fixed case are of a shell nature. A plot of the deformed shape for mode 1, fixed ends with service masses, yields a mode pattern almost identical to that for the model without service mass (Results Figure 6).

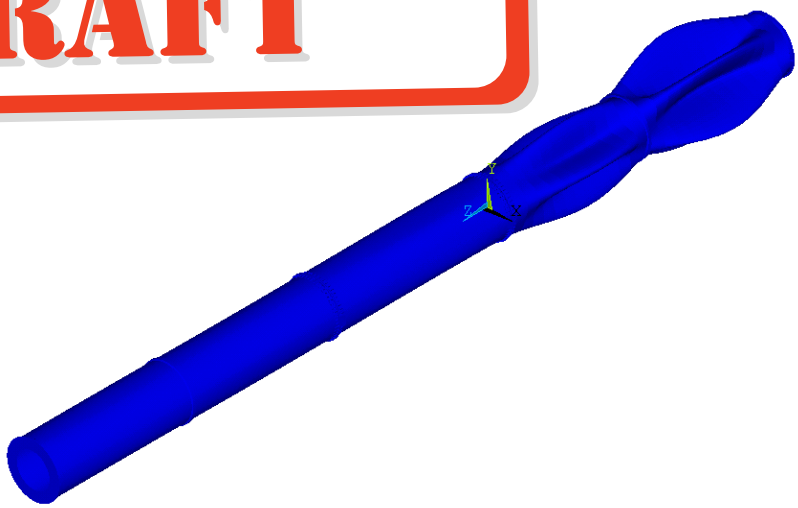

Results Figure 6. Effect of Service Mass in the Forwards.

6.7 Case 7 – Fiberglass Forward Shells

It has recently come under attention that the PST structure, due to its inherent bending stiffness, might impose unwanted loads on the SCT during the unlikely displacement of the cryostat's end from its barrel section. This motion would cause the end of the PST forward to move relative to the SCT, imposing bending loads on the SCT interlinks. There has been a proposal that this displacement may be as large as 2 mm in X or Y (see model coordinate system). In order to mitigate the potential loads that this fault condition would apply, the possibility of fabricating the forward PST shells from fiberglass was investigated. Using a layup similar to that proposed for carbon fiber, a glass laminate would achieve a modulus approximately 20% that of carbon. The fiberglass PST is analyzed to determine vibrational behavior, support reactions under vertical and horizontal bending, and displacements due to gravity sag.

6.7.1 Vibrational Behavior

Initially, the carbon model was analyzed with only the forward shells reduced in stiffness. This change, however, resulted in extremely low frequencies, due to large shell modes in the less stiff forwards. In order to combat this deficiency, additional hoop stiffeners were added at the forwards' quarter points, bringing the number of hoops per forward section to three, instead of one, see Figure 4. This addition improved the frequency significantly, as can be seen in Results Table 7.1. In fact, decreasing the bending stiffness of the PST forwards by almost a factor of five results in frequencies that are reduced by only 20%. This indicates an efficient design, and while the overall frequencies are low (barely more than 40 Hz) this side effect must be accepted if loads on the SCT are to be minimized. (Note that service masses are included in all models, but they are the less conservative 13 kg mass, not the more accurate mass of 17 kg. Also, no free-ended analysis cases are shown, since the approach of decreasing forward shell stiffness eliminates any impetus to leave the forward ends of the PST unconstrained.)

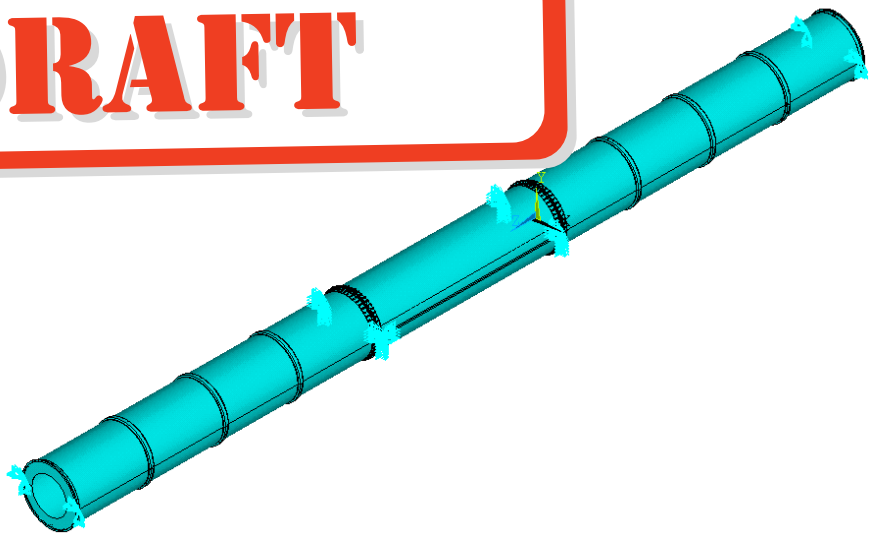

Figure 4. Fiberglass PST with Extra Hoop Stiffeners in Forwards.

Results Table 7.1. Effect of Fiberglass Forwards.
(Shell modes in italics, cantilever modes in bold)

Model Description	Fixed Forwards			
	Mode 1	Mode 2	Mode 3	Mode 4
Carbon Shells – 1 Hoop	*53.1*	*53.2*	*54.2*	*54.2*
Glass Shells – 1 Hoop	*27.4*	*27.4*	*27.8*	*27.9*
Glass Shells – 3 Hoops	*43.7*	*43.7*	*43.8*	*43.8*

6.7.2 Support Reactions

The major concern with PST stiffness is the effect it has on the SCT interlinks (the PST supports) when it undergoes bending. In order to analyze this effect without modeling the SCT, the mount pads on the PST flanges were assumed to be rigidly fixed, according to the fixation scheme explained earlier. The PST forward ends were then displaced by 2 mm in either the vertical or horizontal (and on either one side or both sides). Independent analysis by the SCT group shows that this approximation is not perfect, but it provides a good basis for comparison. Since the PST is mounted only in the horizontal plane, bending of the tube in the vertical is different than bending of the tube in the horizontal, and these two load cases are analyzed independently, with the reactions on the most highly loaded supports shown.

6.7.2.1 Vertical Bending

Since the PST mounts are on the horizontal diameter, vertical bending is far more compliant than bending in the orthogonal direction. For this reason, the loads in vertical bending are fairly low, as shown in Results Table 7.2.1. Both the glass and carbon PST designs are shown for comparison, and displacement is made on *both* ends of the PST. It can be

seen that the glass forwards reduce forces and moments by almost a factor of three.

Results Table 7.2.1. Reaction Loads Under Vertical Bending.

Model Material	FX (N)	FY (N)	FZ (N)	MX (Nm)	MY (Nm)	MZ (Nm)
Carbon	-	151	0	253	-	-
Glass	-	53	0	89	-	-

6.7.2.2 Horizontal Bending

Up to this point, it has not been explicitly stated whether the PST is fixed to the SCT in Z (the beam direction) at only one point. However, all previous analyses have been completely insensitive to this constraint. The horizontal bending analysis, however, is very sensitive to this constraint, as it can apply a large Z load to the SCT during horizontal displacement. The PST has been analyzed with this constraint by the SCT group, and there is concern about the resultant loads. In order to make a comparison here, the PST is analyzed with both 1 and 2 Z constraints at the SCT interlinks (both on side C of the detector). The loads generated here are larger than those generated by the PST analysts, since the models here do not include SCT compliance. The absolute values of these results, therefore, should be viewed with caution. The relative magnitudes, however, should be indicative of the performance advantage of fiberglass forward tubes. In particular, note that the Z force is reduced by a factor of 4 when glass forwards are introduced into the model, Results Table 7.2.2.

Results Table 7.2.2. Reaction Loads Under Horizontal Bending.

Both Sides Bent – 1 Z Constraint						
Model Material	**FX (N)**	**FY (N)**	**FZ (N)**	**MX (Nm)**	**MY (Nm)**	**MZ (Nm)**
Carbon	146	-	-	-	233	-
Glass	52	-	-	-	83	-
Both Sides Bent – 2 Z Constraints						
Model Material	**FX (N)**	**FY (N)**	**FZ (N)**	**MX (Nm)**	**MY (Nm)**	**MZ (Nm)**
Carbon	297	-	1870	-	536	-
Glass	108	-	468	-	110	-
One Side Bent – 1 Z Constraint						
Model Material	**FX (N)**	**FY (N)**	**FZ (N)**	**MX (Nm)**	**MY (Nm)**	**MZ (Nm)**
Carbon	390	-	-	-	623	-
Glass	137	-	-	-	218	-

6.7.3 Gravity Sag

Though less important than the above analysis cases, gravity sag is an important criteria to consider in the PST design, primarily because it determines whether the PST remains inside its envelope during removal and insertion of the SCT

forwards (when the forward ends of the PST are free). Since the pixel detector may at some point remain inside the PST during SCT forward access, it is also important to model the gravity sag with service masses included. In these analyses only, the service masses are modeled as 17 kg per side, which is the more accurate estimation. The results show that the gravity sag for the fiberglass model is less than a factor of 3 greater than that of the carbon one, due primarily to the mount constraints and stiffness of the barrel tube (which is carbon in both models), see Results Figure 7.3. The resultant loads from gravity sag (the same for both models) are also given in Results Table 7.3, and are seen to be reasonable.

Results Table 7.3. Reaction Loads Under Gravity Sag.

Model Material	FX (N)	FY (N)	FZ (N)	MX (Nm)	MY (Nm)	MZ (Nm)
Both	-	110	-	192	-	29

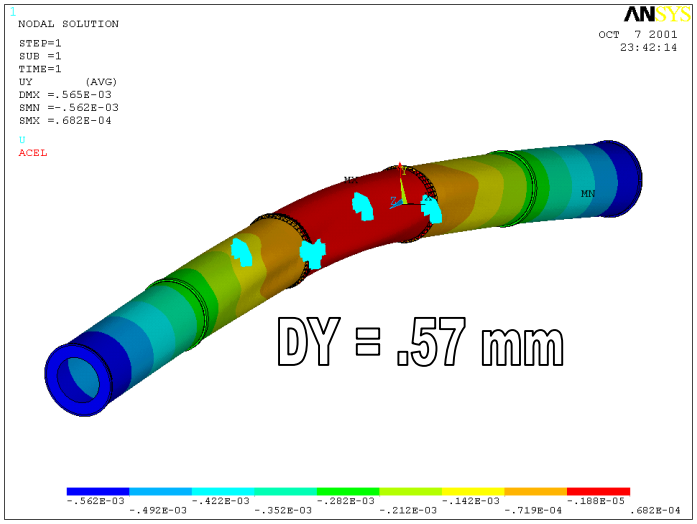

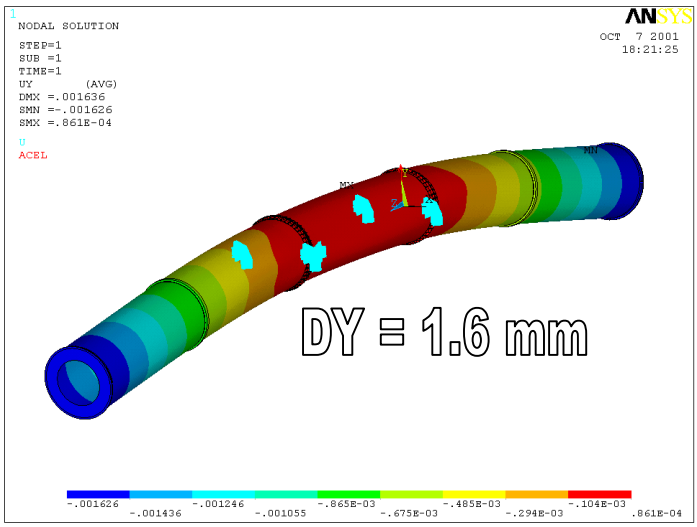

Results Figure 7.3. Displacement Under Gravity Sag (Carbon at Top, Glass at Bottom) - shown in meters.

7.0 Conclusions and Recommendations

The PST design has progressed through a series of iterations in order to arrive at a design that performs adequately well, while allowing maximum flexibility and minimum impact on surrounding detectors. The last design shown above is considered to be a working baseline, and may change in response to concerns that have not been addressed yet. In particular, the effects of possible moments on the SCT interlinks must be addressed (although this effect is mitigated by the support blocks, which will lessen these moments somewhat). Also, the end plugs must be modeled as real structures (rather than the flat plate approximations shown here) and the flanges will change as fabrication designs are worked out. Including service structures, which are stiffer than the distributed mass added to the shells, may also increase frequency somewhat. It will be necessary to work with SCT analysts to answer these questions and any others that may arise.

Appendix 1

Comparison of PST Model Results (Neal H.) to those generated by SCT Analyst (Joel C.)

SCT Analysis Comparisons				
Bend Direction	**Load Case**	**FX (N)**	**FY (N)**	**FZ (N)**
Y	dy1 = dy2 = 2 mm SCT		141	
Y	dy1 = dy2 = 2 mm Carbon		151	
Y	dy1 = dy2 = 2 mm Glass		53	
Y	dy1 = dy2 = 2 mm **Projected***		**49**	
X	dx1 = dx2 = 2mm SCT^	325		588
X	dx1 = dx2 = 2mm Carbon^	297		1870
X	dx1 = dx2 = 2mm Glass^	108		468
X	dx1 = dx2 = 2mm **Projected*^**	**118**		**147**
X	dx1 = 2 mm SCT	462		
X	dx1 = 2 mm Carbon	390		
X	dx1 = 2 mm Glass	137		
X	dx1 = 2 mm **Projected***	**162**		

***Projected values are to be expected when SCT compliance is considered, as it was in SCT models (By Joel C.). These are computed by taking the ratio of SCT result to Carbon result and multiplying by Glass result (all shown above).**

NOTE: These models have two Z constraints (for bending in X), so Z Forces are COMPLETELY ELIMINATED when only 1 Z constraint is used, as is currently proposed.